Chapter 5

Temperature in Machining of Aluminum Alloys

Mário C. Santos, Alisson R. Machado and
Marcos A.S. Barrozo

Additional information is available at the end of the chapter

http://dx.doi.org/10.5772/intechopen.75943

Abstract

The objective this work is to study the effect of the mechanical property of the workpiece (tensile strength) and cutting conditions (cutting speed, feed rate, depth of cut and lubri-cooling system) over the cutting temperature in turning of aluminum alloys. A 2^k factorial planning was used to determine the machining test conditions. ANOVA and Regression Analysis of the results were performed. The main contribution of this work lies on its efficiency of describing the behavior of the cutting temperature as a function of the input variables. The results found in the present work have considered the interactions of the input variables, describing the cutting temperature in a complete way, not seen previously in the literature.

Keywords: cutting temperature, aluminum alloys, factorial planning, machinability, modeling

1. Introduction

Machining of aluminum alloys is an important production activity in the automotive and aeronautical industries, due to the large application of aluminum in the transportation sector [1, 2]. This is because of its great versatility in terms of properties and, among them, its low density and high strength to weight ratio stand out, which makes aluminum, after iron, the materials most used in the manufacture of parts [3–5]. According to Davies et al. [6] the automotive industry is continuously developing technologies to reduce vehicle costs and weights; and with that, reducing the environmental impact with energy consumption. The pressure for reducing vehicle weights has led to the substitution of steel and cast iron for plastic and aluminum to increase fuel economy [7].

Measuring the temperature in the cut region is a complex task due to the difficult access to that region. One of the methodologies that allows its more precise verification is the tool-workpiece thermocouple system, being able to study the variation of the cutting temperature (TC) as a function of many parameters, among them the mechanical strength of the machined alloy and cutting parameters: cutting speed (VC), depth of cut (AP), feed rate (F) and lubri-cooling condition (LUB). With this method, it is possible to determine the variables that most affect the cutting temperature in the secondary shear zone and also generate models to study its behavior.

This chapter will present the fundamentals of the cutting temperature in the machining of aluminum alloys with experimental approach using the tool-workpiece thermocouple system. The methodology that includes details of the collection of voltage signals will also be described. A 2^k factorial planning is used, allowing the analysis of the influences of the input variables on the cutting temperature.

This work is justified due to the ability of the analysis of variance and factorial analysis to investigate the joint influence (simultaneous) of the mechanical strength and cutting conditions (input variables) on the cutting temperature. In machining, few researches have been conducted in this way, since most of them study the influences of the main input variable isolated and rarely considering their interactions in the way conducted here; for instance, the influence of the cutting speed or the feed rate on the cutting forces; the effect of the hardness on the cutting temperature [4, 8, 9]. This greatly limits the discussion about how interactions between inputs variables can affect the responses.

2. Cutting temperature measurement, regression analysis and mathematical modeling

For a better understanding of the behavior of the cutting temperature in the machining of aluminum alloys, the theoretical fundaments will be presented first.

As for the process of temperature measurement in the cutting region, the focus will be on the tool workpiece thermocouple system, when concepts and adaptation of the thermocouple system in the turning process and measuring devices will be presented.

The cutting temperatures will be studied based on the 2^k factorial design, where the input factors will be the mechanical strength of the ALLOYS and cutting parameters: cutting speed (VC), depth of cut (AP), feed rate (F) and lubri-cooling condition (LUB), whose effect on the cutting temperature will be presented based on analysis of variance and factorial effects.

2.1. Fundamentals of the temperature when machining aluminum alloys

The chip formation process involves high deformation rates of the work material (elastoplastic), with almost all the deformation energy converted to heat in the cutting region [10]. This energy can be divided in: (A) – the work to shear the material in the primary shear zone; (B) – the energy needed to plastically deform the chip in the secondary shear zone; (C) – the work required to move the newly formed chip onto the rake surface and (D) – the work involved

in the plastic deformation/friction process in the tertiary shear zone (region where the newly formed surface of the workpiece contacts the clearance face of the tool) [11, 12]. According to Machado et al. [13], the tertiary shear zone is important mainly when using small clearance angles and/or a flank wear has developed, which tend to increase the workpiece-tool contact in the flank region. **Figure 1** shows the four heat generation zones (A, B, C and D).

The heat generated in zones A and B are highly dependent on the cutting conditions and are assumed to be evenly distributed [11]. The portion of heat generated in zone C depends on the kinetic friction of the lower surface of the chip on the tool rake surface and can be assumed linearly decreasing from the end of the adhesion zone to the end of the slipping zone, where no heat is generated any more [11, 14–16]. The amount of heat generated in zone D depends on the clearance angle, flank wear and kinetic friction of the newly machined surface against the tool clearance surface [10, 11, 13].

The energy balance relationship between the heat generated in zones A, B, C and D and the heat dissipated for chip, workpiece, environment and tool, allows the understanding of the energy exchanges involved in the cutting processes [13, 17].

The greater part of the heat generated in zone A is dissipated by the chip, and the part dissipated by the workpiece represents a small portion, which tends to increase under low rates of material removal and at small shear angles, and to reduce at high rates of material removal [12, 13]. These authors make it clear that most of the heat generated in zone B (in the flow zone) goes to the chip and to the tool and because the latter is stationary, it develops high temperatures. The tool temperature is not directly affected by the heat generated in the primary shear zone, since

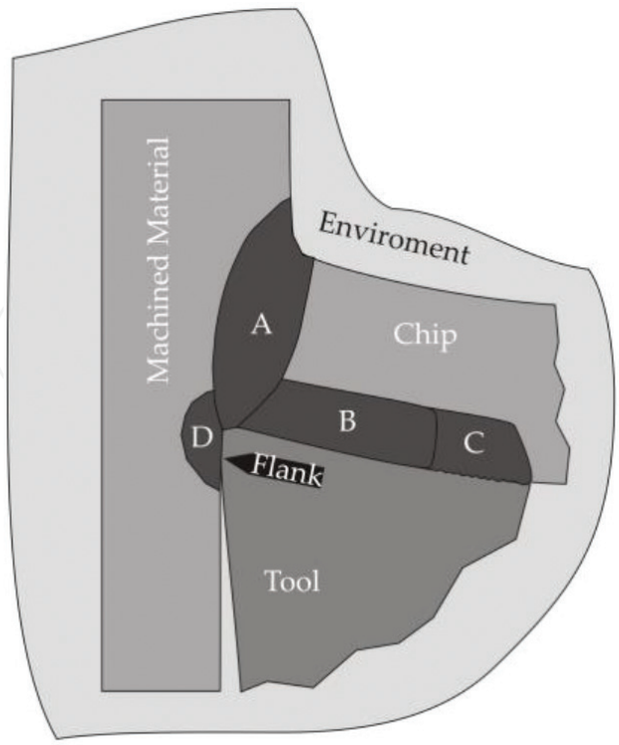

Figure 1. Heat generation zones in machining [13].

the temperature of the secondary shear zone is higher than the temperature of the body of the coming chip. However, indirectly, the heat generated in zone A also contributes to raising and affecting the temperature distribution on the tool wedge.

Researchers have attempted to quantify the heat or temperatures generated in the shear zones. According to Dinc et al. [18], the heat generated in zone A and zone B depends on the cutting speed, shear forces and shear rates in the primary and secondary shear planes.

The mechanical and thermal properties of the work material and the tool, the tool geometry and the cutting conditions have great influence on the generation and transfer of the heat in the thermal zones [11, 12]. The higher the cutting speed, the feed rate and the depth of cut (higher material removal rates), the higher are the machining power and the heat generated in zones A and B [10, 14]; and therefore higher are the temperatures in the cut region [16, 19].

Increasing the cutting speed causes the rate of deformation of the material to increase, especially in zones A and B, which raises the rate of heat generation in these regions. However, the higher the cutting speed, in spite of raising the rate of heat generation in these zones, the lower is the heat flowing from zone A to the workpiece; and from zone B to the cutting tool. Higher feed rates tend to cause greater heat flow from zone B to the tool due to increased stresses and chip-tool contact area. However, Saglam et al. [20] consider that the cutting speed has greater effect on the generation of heat in the shear region than the feed rate. Obviously, the higher the mechanical strength of the work material, the greater the heat generation in zones A and B [9] (increase in the deformation resistance of the material). An efficient cooling action of a cutting fluid can also increase the mechanical resistance of the work material in zones A and B [13], therefore demanding more energy to form the chip and generating more heat. The heat generation in zones (A and B) will largely depend on the thermal conductivity of the tool and work materials and the cooling method [21]. The increase of the rake angle tends to reduce the generation of heat in zones A and B, because it favors the decreasing of the undeformed chip thickness and the slipping process of the chip on the rake face of the tool [9, 13].

Although complex, the temperature prediction at the chip-tool interface is very important in determining the maximum cutting speed, which can be applied in order to avoid reaching critical temperature levels. In the drilling of the aluminum Alloy 319 (5.5–6.5% Si), Dasch et al. [22] recorded a carbon coating impairment (DLC: Diamond Like Carbon) of the tool, at shear temperatures greater than 350°C, which caused clogging of the drill channels, due to the softening of the metal.

The great problem of temperature is when machining of aluminum alloy that have hard particles, such as the hypereutectic alloys of Si (17% and 23% Si), whose shear temperatures are quite high due to the constant friction of the large particles of Si precipitates (average diameter 70 μm, melting temperature of 1420°C and hardness greater than 400 HV) on the rake and clearance surfaces of the cutting tools [21]. In the dry turning of the aluminum alloys LM28 (17% Si) and LM13 (12% Si), in the proportion that the cutting speed was increased, higher cutting temperatures were registered in the first, due to their higher Si content and hardness and lower thermal conductivity [23]. In these same alloys, in the cast, cast/refined and thermally treated (T6) conditions, this (higher resistance limit) provided higher temperatures, agreeing with [21, 24].

In the milling of A356 aluminum alloy, the increase in cutting temperature was observed with increasing cutting speed, which increased the amount of material adhered to the workpiece surface and to the cutting edge of the tool [25]. Kiliçkap et al. [26], during turning of Al-pure (5% SiC), also observed the increase of the temperature with the increase of the feed rate, which caused the weakening of the bond between the SiC particles and the aluminum matrix. Simulations by Zaghbani and Songmene [24], during the milling of the 7075-T6 aluminum alloy, showed the increase of the cutting temperature with the increase of the cutting speed and the feed; however, with the latter, the temperature increased asymptotically. This was explained by the increase in the rate of deformation with the increase of the cutting speed and its reduction with the increase of the feed rate.

Large rake angles, low coefficient of friction at the chip-tool contact and the presence of free cutting elements favor the chip flow on the surface of the tool (smaller cutting forces); and therefore inhibit the excessive elevation of the cutting temperature [16, 21, 27]. In the drilling of the aluminum alloy 319 (with 0.17% Pb), temperatures of the order of 375°C was obtained by infrared images; while in the same alloy without Pb, the level of temperature found was 450°C [28].

Geometric changes, such as those provided by flank wear, increase the cutting forces, which, in turn, increase the cutting temperature. During milling of the 7050-T7451 aluminum alloy, increased cutting forces was noticed with increased flank wear, which the consequent increase in cutting temperature helped to promote [29]. In this respect, Machado et al. [13] consider that if a tool achieves a considerable level of flank wear, the heat generated by zone D becomes prominent due to the intense forces that will appear in that region.

2.2. Thermocouple systems

Several methods have been developed for measuring the cutting temperature [13], but the tool-workpiece thermocouple method, according to Da Silva and Wallbank [12] and GrzesiK [30], is the most used to predict the effect of the cutting conditions on the chip-tool interface temperature. The method uses the principle that a metal, subjected to a temperature differential, undergoes a non-uniform free electron distribution, which consequently causes an electromotive force differential – a phenomenon known as the Seebeck effect [31].

The practical use of the Seebeck effect in the measurement of a certain temperature (TJ) requires the use of two metallic materials (A and B), with different Seebeck coefficients, as shown in **Figure 2** (basic thermocouple circuit). In it, numbers 1, 2 and 3 are, respectively, the junctions between the elements of the circuit.

Since the connection elements of the voltmeter (1 and 3) are at the same temperature (TT), it can be proved, via a path integral along the circuit of **Figure 2**, that its fundamental electromotive force (EAB) equation is given by:

$$EAB = \int_{TT}^{TJ} \sigma abdT \tag{1}$$

Thus, σab is the difference between the Seebeck coefficients of the thermocouple materials (A) and (B); and EAB is the electromotive force induced by the gradient between the desired temperature (TJ) (hot junction) and the temperature (TT) (cold junction).

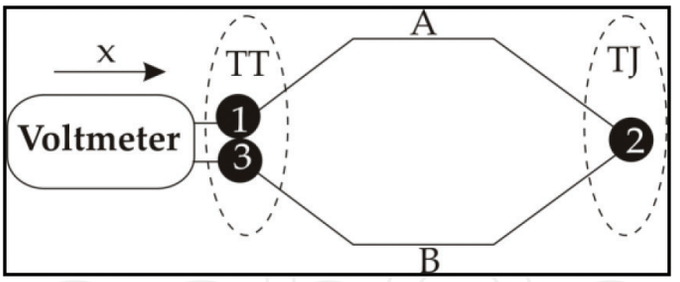

Figure 2. A basic thermocouple circuit [31].

It is possible to establish a reference temperature (TR) equal to zero by the arrangement of the electric circuit of thermocouples of **Figure 3**. In this figure, TR and TT are any temperatures; TJ is the desired temperature (hot junction of the thermocouple) – the numbered dark points are the junctions between the elements of the electric circuit, which allow its continuity.

The electromotive forces due to copper wires cancel out. Through a suitable calibration process involving the desired temperature (TJ) and the electromotive force of the circuit (E0J), it is possible to establish a mathematical relationship between these quantities:

$$TJ = G(E0J) = b_0 + b_{1*} E_{0J} + b_{2*} E^2{}_{0J} + \ldots + b_n E^n{}_{0J} \quad (2)$$

2.3. The tool-workpiece thermocouple system for measuring the cutting temperature

Figure 4 shows a schematic draw of the tool-workpiece thermocouple system used in the process of acquisition of electromotive force (FEM), during the machining. The multimeter (11) and wires (8–9) should be the same as those used in the calibration process of the tool-workpiece thermocouple; the tool holder (13) is isolated from the structure of the CNC lathe with celeron plates (2 mm) around it. Three brushes (7) allow to close the electric circuit of the system, with the workpiece (3) in rotating movement, in the presence of a thin layer of solid Vaseline in their contacts. With the exception of the tool holder/cutting tool and the workpiece, the CNC lathe and accessories are connected to the equipotential earth (14).

Figure 5 shows schematically the thermoelectric junctions present in the electrical circuit of **Figure 4**, where J1 is the junction copper wire (8) – connector multimeter; J2 is the junction tool (13) – copper wire (8); J3 is junction tool (13) – workpiece (3); J4 is the junction workpiece

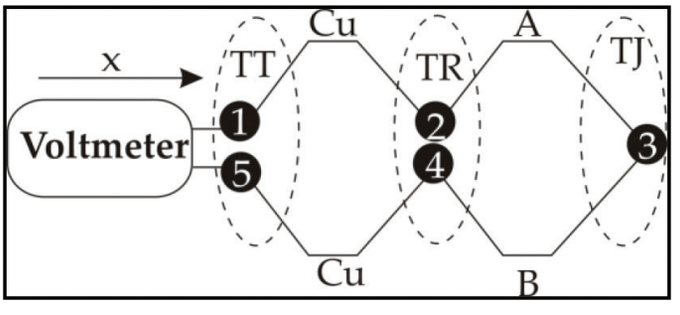

Figure 3. Thermocouple circuit with a zero reference temperature [31].

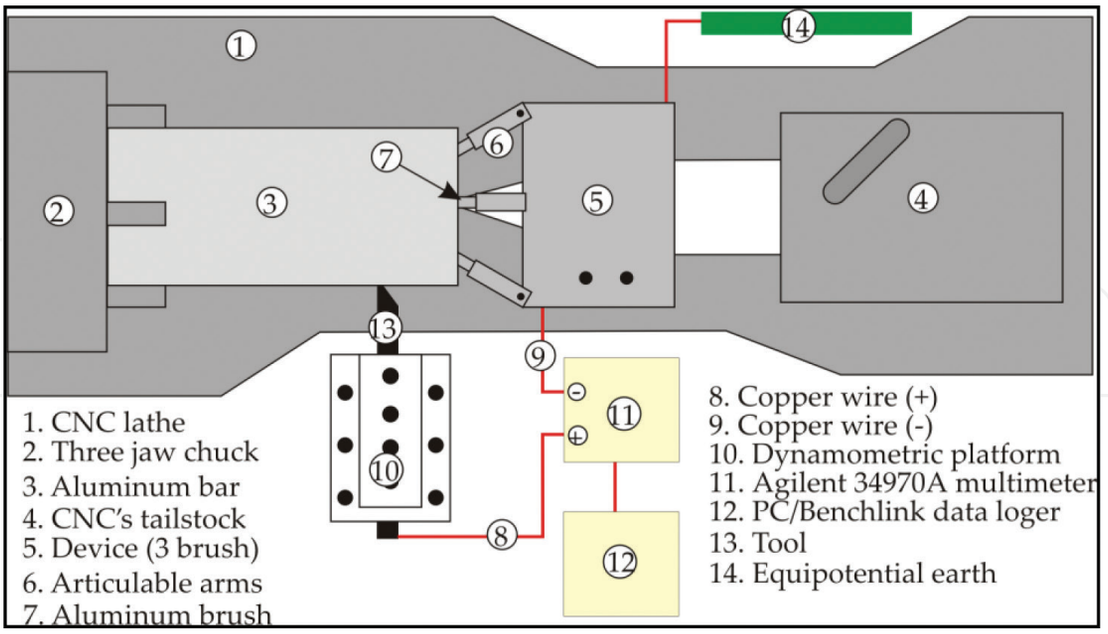

Figure 4. Schematic draw of the tool-workpiece thermocouple system.

(3) – brushes (7); J5 is the junction brushes (7) – articulating arm (6); J6 is the junction articulating arm (6) – device body (5); J7 is the junction device body (5) – copper wire (9); and J8 is the junction copper wire (9) – multimeter connector.

During machining, the electromotive force generated in the tool-workpiece thermocouple circuit is proportional to the temperature gradient between the tool and the room temperature. The metal segments between junctions 1–2 and 4–5, because they are at the same temperature, do not generate electromotive forces. Thus, the only pairs of junctions, which are under temperature gradient and therefore contribute to the electromotive force of the electric circuit are the pairs of joints 2–3 and 3–4.

2.4. The temperature measurement device in turning process

For cutting temperature measurement in turning with the tool-workpiece thermocouple system, it is necessary to develop a device analogous to the one shown in **Figure 4**. Two important

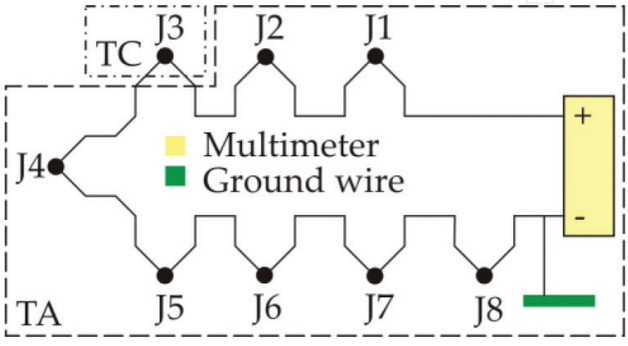

Figure 5. The thermoelectric junctions of the electrical circuit.

connection components are required for completing the electric circuit and capture the electromotive forces, the tool (13) and the 03 brushes device of **Figure 4**.

2.4.1. The three brushes device

Figure 6 shows details of the three brush device, element (5) of **Figure 4**: (1) body of the device; (2) tailstock gulf; (3) articulating arm, with central bore; (4) workpiece bar; (5) wire connectors; (6) aluminum brush. With the exception of the springs inside the articulating arms and screws, all the elements were made of aluminum alloy.

2.4.2. The tool and tool holder

Figure 7 shows an image of the cutting tool ((13) in **Figure 4**), adapted for measuring the cutting temperature (TC) in the turning process: (1) is the cemented carbide bit (310 × 10 × 4 mm); (2) is the tool holder (25 × 20 × 150 mm) made of steel; (3) are the fastening screws of the carbide bar in the tool holder; (4) is the lateral electrical insulation; (5) is the upper electrical insulation; (6) is the lower electrical insulation; (7) is the copper connector. Through this element the tool was connected to the multimeter through a copper wire.

2.4.3. Machinery, tools and consumables

The cutting temperature tests were carried out on a CNC lathe, model Multiplic 35D, manufactured by ROMI. The cutting tool was a rectangular carbide bar (13 × 4 × 310 mm) K15 grade, with 93% WC + 7% Co, grain size 1.0 μm and hardness of 1580 HV (TASK, 2009). Its geometry was ground in one of its ends, as presented in **Figure 8**.

The cutting fluid applying by flooding was the water miscible (Vasco 1000 – Blaser Swisslube) – high performance biodegradable oil, recommended for machining non-ferrous materials, with 45% vegetable oil (no mineral based oil), 0.1% H_2O, density of 950 kg/m^3 (20°C), viscosity of 56 mm^2/s (40°C) and flash point of 180°C (BLASER SWISSLUBE, 2010). The fluid was applied at the cutting region with a concentration of 6% in water (frequently checked with an ATAGO refractometer) and a flow rate of 360 L/h.

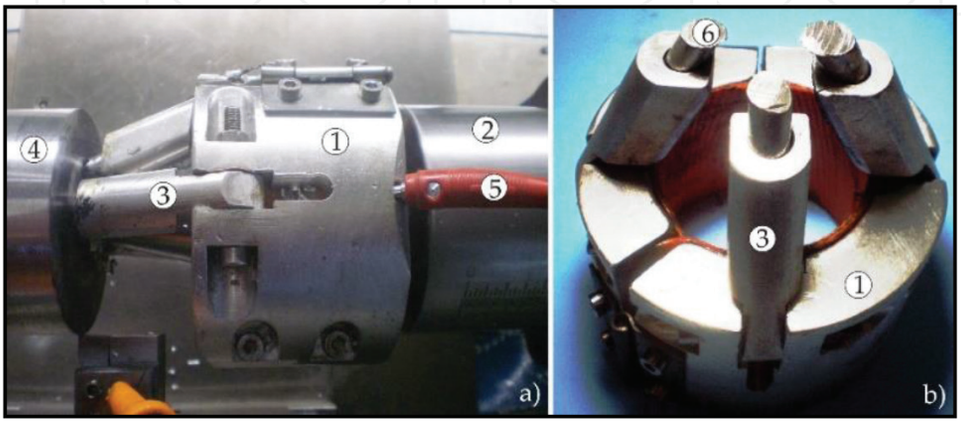

Figure 6. The three brushes device used for temperature measurement in turning.

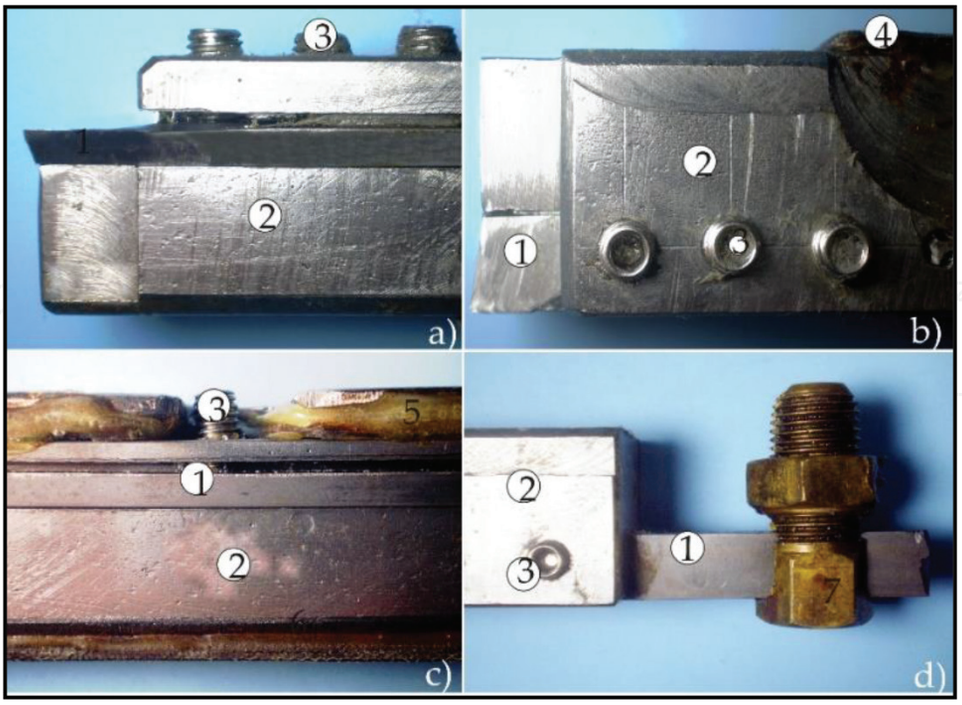

Figure 7. Photos of the cutting tool: (a) lateral view; (b) superior view; (c) lateral view of the mid of the tool holder; (d) superior view of the opposite end.

2.5. The 2^k factorial design

In this case study, the effect of five (k = 5) input parameters (Tensile strength of the workpiece – ALLOY, cutting speed (VC), depth of cut (AP), feed rate(F) and lubri-cooling condition (LUB) on the cutting temperature collected with the methodology of the tool-workpiece thermocouple system presented in **Figure 4** will be considered.

2.5.1. The levels of the input variables

Table 1 shows the levels of the factors that combined, resulted in 32 treatments (tests) for studying the cutting temperature in turning of aluminum alloys.

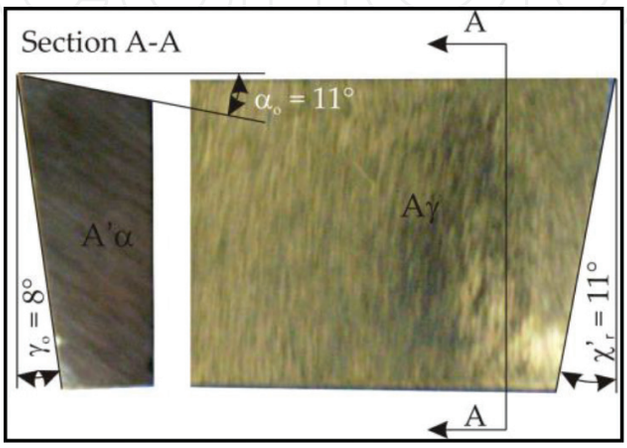

Figure 8. Tool bit geometry.

Level	Alloy	VC (m/min)	F (mm/rot)	AP (mm)	LUB
Low (−1)	1350-O	300	0.2	1	Dry
High (+1)	7075-T6	600	0.3	3	Flood

Table 1. Level of the factors of the 2^k factorial design.

The workpiece was extruded round bars (Ø 101 × 2000 mm) of the following aluminum alloys: 1350-O and 7075-T6; manufactured by Alcoa. **Table 2** shows the chemical composition, highlighting the main chemical elements present in the aluminum alloys.

Figure 9a and **9b** show micrographs for the 1350-O and 7075-T6 alloys, respectively. Intermetallic precipitates of $FeAl_3$, AlFeSi, and Mg_2Al due to the annealing process can be identified (**Figure 9a**), while the matrix of the 7075-T6 alloy (**Figure 9b**) exhibits a high density of

Elements	1350-O	7075
Cu	0.05	1.20–2.00
Fe	0.40	0.05
Mg	0.03	2.10–2.90
Mn	0.10	0.30
Ni	0.03	0.05
Si	0.10	0.40
Ti	0.03	0.20
Zn	0.05	5.10–6.10
Bi	0.03	0.05
Cr	0.01	0.18–0.28
Pb	0.03	0.050
Sn	0.03	0.05
Be	0.03	0.05
Ca	0.03	0.05
Ga	0.03	0.05
Li	0.03	0.05
Na	0.03	0.05
Sr	0.03	0.05
Zr	0.03	0.05
Others	0.10	0.15
Al	Rem.	Rem.

Table 2. Chemical composition (wt %) of the aluminum alloys.

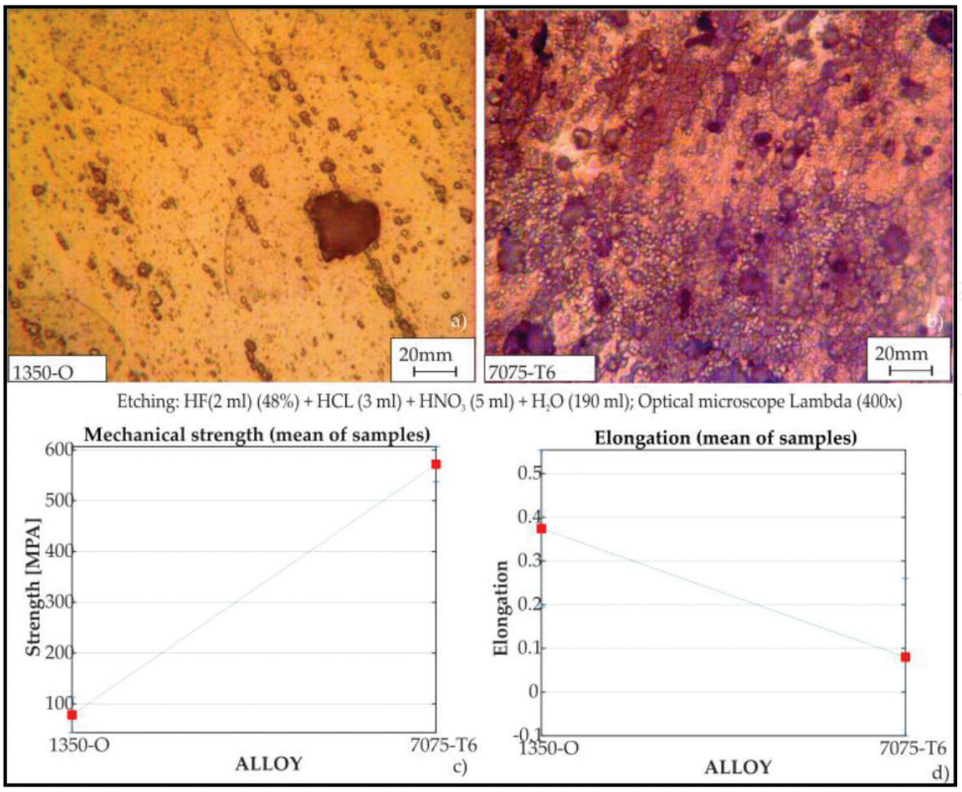

Figure 9. (a) Microstructure of the 1350-O alloy; (b) microstructure of the 7075-T6 alloy; (c) mechanical strength of the alloys; (d) elongation of the alloys.

fine $MgZn_2$ precipitates as a result of the artificial aging process that provides a high mechanical strength relative to the 1350-O alloy. **Figure 9c** and **9d** show mechanical strength of the alloys and elongation of the alloys, respectively.

2.6. Temperature measurement

Table 3 presents the results of the chip-tool temperatures (TC) measured (average of two replicates) by the tool workpiece thermocouple system according to the 2^k factorial design using as input variables: ALLOY, VC, AP, F and LUB.

2.7. Temperature results analysis

2.7.1. Analysis of variance (ANOVA)

Table 4 presents the statistic analysis (ANOVA) of the chip-tool interface temperature considering the 32 tests, where the effects of the main significant input parameters are identified (p value <0.05) with 95% of confidence level. Observe that ALLOY, VC, and AP either individually or in interactions appear with significant influences on the temperature according to the ANOVA.

Alloy	VC	AP	F	LUB	TC (°)
−1	−1	1	−1	−1	282.84
−1	1	1	−1	−1	362.02
−1	−1	1	1	−1	238.39
−1	1	1	1	−1	277.97
−1	−1	−1	−1	−1	333.17
−1	1	−1	−1	−1	417.85
−1	−1	−1	1	−1	345.87
−1	1	−1	1	−1	429.45
−1	−1	1	−1	1	339.64
−1	1	1	−1	1	405.27
−1	−1	1	1	1	307.62
−1	1	1	1	1	406.61
−1	−1	−1	−1	1	314.54
−1	1	−1	−1	1	400.05
−1	−1	−1	1	1	323.80
−1	1	−1	1	1	418.39
1	−1	1	−1	−1	580.68
1	1	1	−1	−1	633.02
1	−1	1	1	−1	575.51
1	1	1	1	−1	641.39
1	−1	−1	−1	−1	564.23
1	1	−1	−1	−1	639.80
1	−1	−1	1	−1	588.98
1	1	−1	1	−1	652.00
1	−1	1	−1	1	573.68
1	1	1	−1	1	635.63
1	−1	1	1	1	591.46
1	1	1	1	1	647.10
1	−1	−1	−1	1	564.37
1	1	−1	−1	1	637.41
1	−1	−1	1	1	586.82
1	1	-1	1	1	653.54

Table 3. Average results of the chip-tool interface temperature of the 2^k factorial design.

	R^2	0.97	FStat	212.617	pValModel	3.20E-20
Source of variation	**SQ**	**GL**	**MQ**	**Coef**	**Fstat**	**p Value**
ALLOY	541359.56	1.00	541359.56	130.07	966.73	0.00
VC	41034.95	1.00	41034.95	35.81	73.28	0.00
AP	4311.41	1.00	4311.41	−11.61	7.70	0.01
ALLOY×AP	3917.59	1.00	3917.59	11.06	7.00	0.01
AP×LUB	4694.76	1.00	4694.76	12.11	8.38	0.01
Error	14559.77	26.00	559.99	'GLR'	5.00	—
Total	609878.03	31.00	'SQR'	595318.27	'MQR'	119063.65

Table 4. Analysis of variance of the 2^k factorial design.

2.7.2. Verification of the suitability of the ANOVA models of the 2^K factorial design

Analysis of the residues of the models used in the analysis of variance (ANOVA) of the factorial planning was carried out, by verifying the expected value of the residue (**Figure 10a**), which showed them randomly distributed around zero, which indicates the suitability of the ANOVA models. **Figure 10b**, compare observed value (Yobs) e predicted value (Ypred) which shows close proximity to each other.

2.7.3. Effects of the input variables

Figures 11 and **12** show the graphics of tendencies of the effects of the input variables on the cutting temperature. When increasing the depth of cut from 1 mm (low level) to 3 mm (high level) the chip-tool interface temperature decreases (**Figure 11a**). Although increasing the depth of cut tends to increase the machining forces, a better heat dissipation could have occurred with the increase of the cutting area, which caused a reduction of the cutting

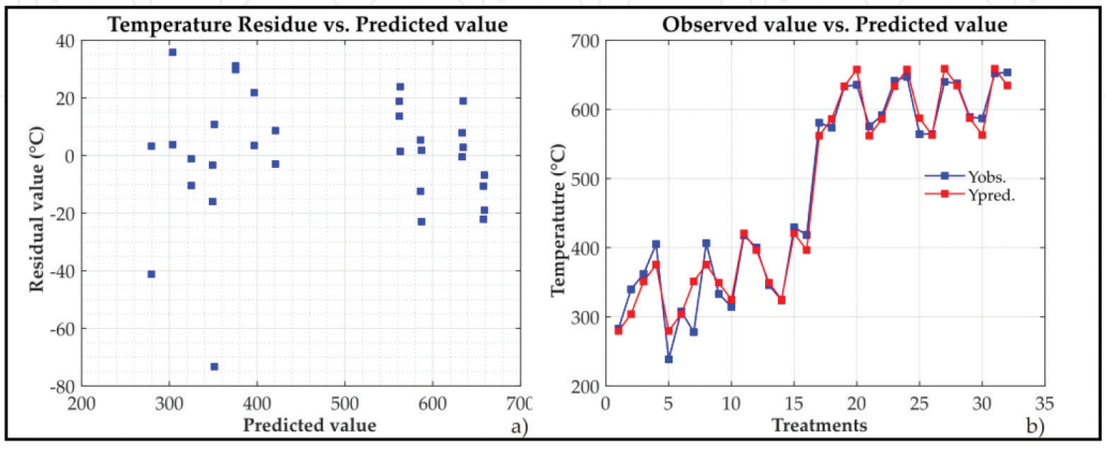

Figure 10. (a) Residues vs. predicted values; (b) predicted values (Ypred) vs. observed values (Yobs).

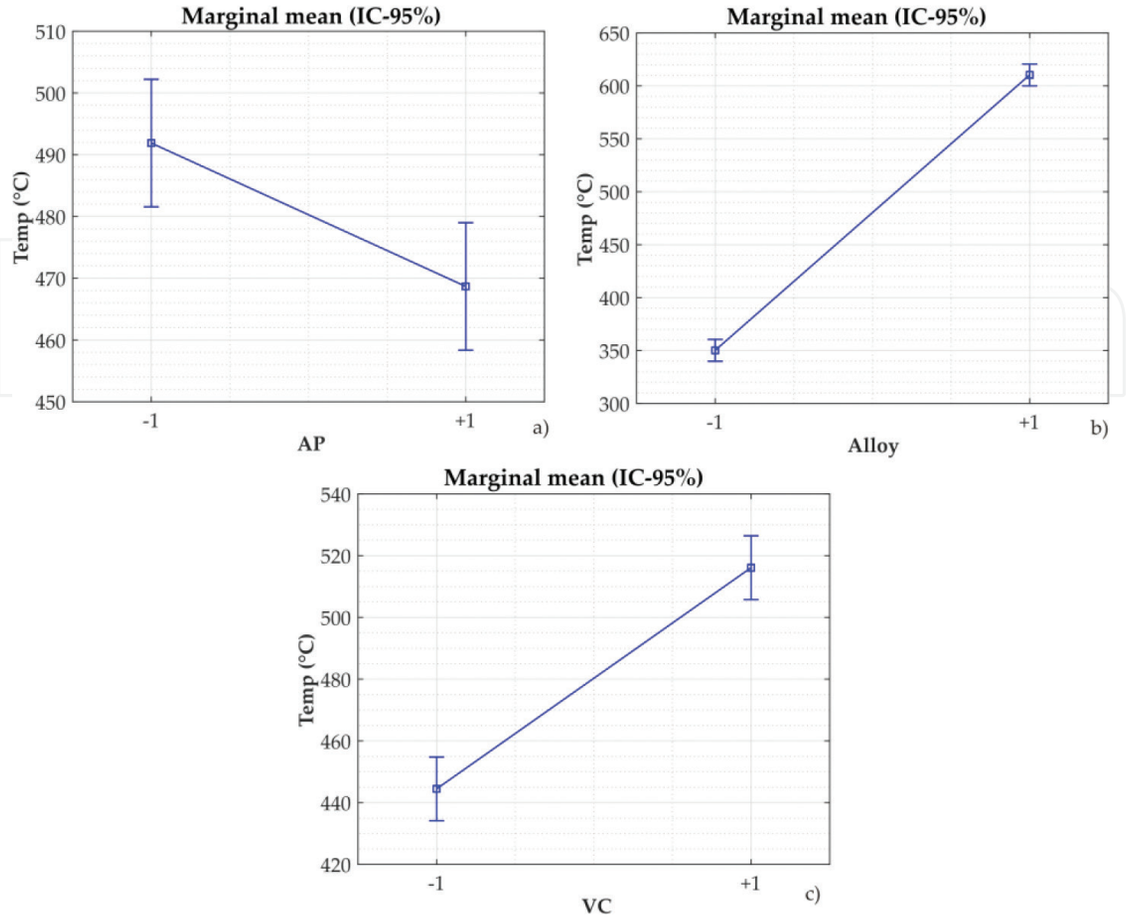

Figure 11. Behavior of the cutting temperature when changing the: (a) depth of cut (AP); (b) ALLOY; (c) cutting speed (VC).

temperature. **Figure 11b** shows that when changing the aluminum alloy from the high ductile 1350-O to the less ductile 7075-T6, the chip-tool interface temperature raised. This is because the higher shear strength of the 7075-T6 alloy, as compared to the 1350-O. **Figure 11c** shows that increasing the cutting speed increased the cutting temperature because it increased the shear rate in the cutting region.

Figure 12a shows effect of the interaction between the depth of cut (AP) and lubri-cooling condition (LUB) on the cutting temperature. When using flood cooling (LUB+1) and the depth of cut of 1 mm (level −1) the average temperature at the chip-tool interface was about 10°C lower than dry condition. However, when the depth of cut of 3 mm (level +1) was used, the temperature was higher (about 40°C) when using the flood cooling than when cutting dry. This is, perhaps, because the cooling action of the cutting fluid was more important than its lubricating action, thereby increasing the shearing strength of the work material in the cutting region, which was also favored by the increase in the areas of these planes (AP level +1), which in turn has improved the heat dissipation in the cutting region. In **Figure 12b**, the interaction between the ALLOY (strength) and the depth of cut (AP) is illustrated. When changing from 1350-O ALLOY (level -1) to ALLOY 7075-T (level +1) there was a great increase in shear strength in the shear planes and thus an increase of the heat generation and cutting temperature.

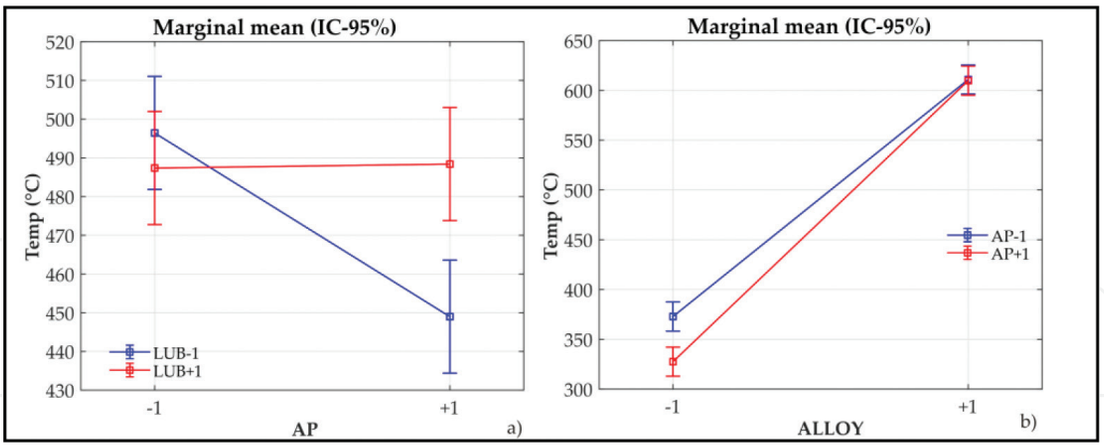

Figure 12. Effect of the interaction of input variables in the cutting temperature: (a) depth of cut (AP) and lubri-cooling condition (LUB); (b) ALLOY and depth of cut (AP).

3. Conclusions

The measurement of the cutting temperature with the tool-workpiece thermocouple system with the 03 brushes device allowed the investigation of the influences of the cutting conditions (VC, AP, and LUB) and the mechanical strength of the aluminum alloy (ALLOY) over the cutting temperature (TC). It was verified that the cutting temperature was greatly affected by the individual variation of the factors (ALLOY, VC, AP, LUB), as well as by their interactions. It was observed an increase in the cutting temperature with increasing cutting speed and mechanical strength of the ALLOY. The cutting temperature decreased with increasing depth of cut. The interaction of increasing ALLOY strength and depth of cut also increased the cutting temperature. The effect of the application of a cutting fluid depended on the depth of cut used. With the lower level of doc (1 mm) the cutting fluid reduced the cutting temperature when compare to dry cutting. This did not occur when using the high level of doc (3 mm), where the cutting fluid increased the chip-tool interface temperature, probably because it increased the shear strength of the work material by cooling the cutting region. The direction of growth of the cutting temperature occurred with the increase of the depth of cut, the advance and the cutting speed, having this greater effect.

Acknowledgements

The authors are grateful to CNPq, CAPES and FAPEMIG for usual financial support to LEPU – Laboratory for Education and Research in Machining – UFU.

Conflict of interest

The authors declare that no 'conflict of interest' whatsoever exists in publishing this book chapter.

Appendices and nomenclature

A_α	relief surface
A_γ	rake surface
AP	depth of cut (mm)
Coef	model coefficients
IC	confidence interval
Cu	copper
F	feed rate (mm/rev)
Fstat	statistics F of the coefficient
FEM	electromotive force (V)
GL	degree of freedom
LUB	lubri-cooling condition
MQR	quadratic mean of the model
p-value	statistic p of the coefficient
pValModel	statistic p of the model
R^2	determination coefficient
SQ	quadratic sum of the coefficient
SQR	quadratic sum of the model
TA	room temperature (°C)
TC	cutting temperature (°C)
TR	reference temperature (°C)
TJ	junction temperature
TT	cold junction temperature
VC	cutting speed (m/min)
χ'_r	approach angle
α_o	relief angel
γ_o	rake angle

Author details

Mário C. Santos[1]*, Alisson R. Machado[2,3] and Marcos A.S. Barrozo[4]

*Address all correspondence to: mcezarjr@ifes.edu.br

1 Mechanical Engineering Department, Federal Institute of Technology of Espírito Santo, São Mateus, ES, Brazil

2 Universidade Católica do Paraná—PUCPR, Curitiba, PR, Brazil

3 Faculty of Mechanical Engineering, Federal University of Uberlandia, Uberlandia, MG, Brazil

4 Faculty of Chemical Engineering, Federal University of Uberlandia, Uberlandia, MG, Brazil

References

[1] Hovsepian PE, Luo Q, Robinson G, Pittman M, Howarth M, Doerwald D, Tietema R, Sim WM, Deeming A, Zeus T. TiAlN/VN superlattice structured PVD coatings: A new alternative in machining of aluminium alloys for aerospace and automotive components. Surface and Coating Technology. 2006;**201**:265-272

[2] Demir H, Gündüz S. The effects of aging on machinability of 6061 aluminium alloy. Journal Materials and Design. 2009;**30**:1480-1483

[3] Figueiredo KM. Mapeamento dos modos de transferência metálica na soldagem de alumínio [thesis]. Uberlância: Universidade Federal de Uberlândia, Uberlândia; 2000

[4] Hamade RF, Ismail F. A case for aggressive drilling of aluminum. Journal of Materials Processing Technology. 2005;**166**:86-97

[5] Roy P, Sarangi SK, Ghosh A, Chattopadhyay AK. Machinability study of pure aluminium and Al–12% Si alloys against uncoated and coated carbide inserts. International Journal of Refractory Metals & Hard Materials. 2009;**27**:535-544

[6] Davies RW, Vetrano JS, Smith MT, Pitman SG. Mechanical properties of aluminum tailor welded blanks at superplastic temperatures. Journal of Materials Processing Technology. 2002;**128**:38-47

[7] Miller WS, Zhuang L, Bottema J, Wittebrood AJ, De Smet P, Haszler A, Vieregge A. Recent development in aluminium alloys for the automotive industry. Materials Science and Engineering. 2000;**280**:37-49

[8] Manna A, Bhattacharyya B. A study on different tooling systems during machining of Al/SiC-MMC. Journal of Materials Processing Technology. 2002;**123**:476-482

[9] Vernaza-Pefia KM, Mason JJ, Li M. Experimental study of the temperature field generated during orthogonal machining of an aluminum alloy. Experimental Mechanics. 2002;**42**:221-229

[10] Seker U, Korkut İ, Turgut Y, Boy M. The Measurement of Temperature During Machining. International Conference Power Transmissions; 2003

[11] Abukhshim NA, Mativenga PT, Sheikh MA. Heat generation and temperature prediction in metal cutting: A review and implications for high speed machining. International Journal of Machine Tools & Manufacture. 2006;**46**:782-800

[12] Da Silva MB, Wallbank J. Cutting temperature: Prediction and measurement methods—A review. Journal of Materials Processing Technology. 1999;**88**:195-202

[13] Machado AR, Abrão AM, Coelho RT, Da Silva MB. Teoria da usinagem dos metais. São Paulo: Edgard Blucher; 2009. 751 p

[14] Boothroyd G. Fundamentals of Metal Machining and Machine Tools. London: McGraw-Hill Internacional Bool Company; 1981

[15] Diniz AE, Marcondes FC, Coppini NL. Tecnologia da Usinagem dos Metais. 3nd ed. São Paulo: Artliber; 2001

[16] Mills B, Redford AH. Machinabilitty of Engineering Materials. London: Applied Science Publishers; 1983. DOI: 10.1007/978-94-009-6631-4

[17] Astakhov VP. Tribology of Metal Cutting. London: Elsevier; 2006

[18] Dinc C, Lazoglu I, Serpenguzel A. Analysis of thermal fields in orthogonal machining with infrared imaging. Journal of Materials Processing Technology. 2008;**198**:147-154

[19] Dimla E, Dimla SNR. Sensor signals for tool-wear monitoring in metal cutting operations—A review of methods. International Journal of Machine Tools & Manufacture. 2000;**40**:1073-1098

[20] Saglam H, Unsacar F, Yaldiz S. Investigation of the effect of rake angle and approaching angle on main cutting force and tool tip temperature. International Journal of Machine Tools & Manufacture. 2006;**46**:132-141

[21] Trent EM, Wright PK. Metal Cutting. 4nd ed. Boston: Butterworth Heinemann; 2000 439 p

[22] Dasch JM, Ang CC, Wong CA, Cheng YT, Weiner AM, Lev LC, Konca E. A comparison of five categories of carbon-based tool coatings for dry drilling of aluminum. Surface and Coating Technology. 2006;**200**:2970-2977

[23] Dwivedi DK, Sharma A, Rajan TV. Machining of LM13 and LM28 cast aluminium alloys: Part I. Journal of Materials Processing Technology. 2008;**196**:197-204

[24] Zaghbani I, Songmene V. A force-temperature model including a constitutive law for dry high speed milling of aluminium alloys. Journal of Materials Processing Technology. 2009;**209**:2532-2544

[25] Kishawy HA, Dumitrescu M, Ng EG, Elbestawi MA. Effect of coolant strategy on tool performance, chip morphology and surface quality during high-speed machining of A356 aluminum alloy. International Journal of Machine Tools & Manufacture. 2005;**45**:219-227

[26] Kiliçkap E, Çakir OC, Aksoy M, Inan A. Study of tool wear and surface roughness in machining of homogenized SiC-p reinforced aluminium metal matrix composite. Journal of Materials Processing Technology. 2005;**164-165**:862-867

[27] Fukui H, Okida J, Omori N, Moriguchi H, Tsuda K. Cutting performance of DLC coated tools in dry machining aluminum alloys. Surface and Coating Technology. 2004;**187**:70-76

[28] Dasch JM, Ang CC, Wong CA, Waldo RA, Chester D, Cheng YT, Powell BR, Weiner AM, Konca E. The effect of free-machining elements on dry machining of B319 aluminum alloy. Journal of Materials Processing Technology. 2009;**209**:4638-4644

[29] Tang ZT, Liu ZQ, Pan YZ, Wan Y, Ai X. The influence of tool flank wear on residual stresses induced by milling aluminum alloy. Journal of Materials Processing Technology. 2009;**209**:4502-4508

[30] Grzesik W. Experimental investigation of the cutting temperature when turning with coated indexable inserts. International Journal of Machine Tools & Manufacture. 1999;**39**: 355-369

[31] Recktenwald G. Conversion of Thermocouple Voltage to Temperature. Portland: Portland State University; 2010. 23 p

IntechOpen